

Correlation between building damage, ground motion parameters and input energy: a novel ranking scheme using multivariate analysis

Chenna Rajaram^{1,*} and R. Pradeep Kumar²

¹Department of Civil Engineering, Rajeev Gandhi Memorial College of Engineering and Technology, Nandyal 518 501, India

²Earthquake Engineering Research Centre, International Institute of Information Technology, Hyderabad 500 032, India

The present study describes the interdependency between earthquake ground motion parameters and seismic damage to various buildings. A novel ranking procedure between energy, damage and seismic risk has been proposed for buildings subjected to ground motions. Correlation analysis was done between damage to buildings, energy and total energy to confirm the trend of parameters and their influence on total energy ranking. It was found that high peak ground acceleration (PGA) or high energy alone may not lead to extensive damage to the buildings. However, they were affected by the predominant frequency, duration of ground motion and amplitude. A correlation study was performed using over 300 ground motions datasets. It was found that the seismic damage of low-rise buildings had a moderate correlation with root mean square acceleration, characteristic intensity, sustained maximum acceleration and effective design acceleration. Also, a weak correlation was observed between seismic damage of high-rise, tall buildings and $(V/H)_{PGA}$, A_{rms} . The damage and seismic risk rankings may help change Government policies for retrofitting buildings.

Keywords: Buildings, ground motion parameters, multivariate analysis, seismic risk.

SEISMIC risk (R) analysis plays a vital role in the urban planning and development of a city. It is defined as the product of the expected seismic hazard (H) of an area, the number of persons exposed to the seismic hazard (E) and the known vulnerability of the built environment of the area (V). The seismic hazard of an area can be estimated through either deterministic or probabilistic analysis. It may depend on seismic faults and regional site-specific geological and geotechnical features. Predicting structural damage and estimating seismic hazard play a vital role in seismic risk assessment. The ground acceleration time history consists of inherent information that can be extracted through computer analysis, and the results can be classified as (i) Ground motion parameters (GMPs), (ii) spectral parameters, and (iii) energy parameters. Table 1 explains these param-

eters. Though peak ground acceleration (PGA) is a crucial parameter to characterize the seismic damage of structures, the scope of its application is limited because it only provides the maximum force demand but not the frequency at which that force is acting and its duration. However, PGA is widely used because of its simplicity.

Being an important ground-motion parameter, PGA has a low correlation with seismic damage to reinforced concrete (RC) buildings, among other parameters¹⁻³. In addition to PGA, other ground-motion parameters also cause damage to structures. After severe earthquakes in the past, the structural response of damaged buildings was correlated with GMPs, spectral parameters and energy parameters⁴. The dependency of these parameters on the behaviour of RC frame structures has been expressed in the form of correlation coefficients⁵. Therefore, a single parameter like PGA cannot describe the seismic damage to a structure. Other parameters such as Arias intensity, energy response spectra and strong motion duration can cause damage to structures⁶⁻⁸. In general, the seismic performance of any structure is described by maximum inter-storey drift. Studies have been conducted to examine the correlation between the inter-storey drift of framed structures and the intensity of ground motion^{1,9}. However, they ignored structure characteristics and soil-structure interaction (SSI)¹⁰. Kamal and Inel¹¹ studied the relation between GMP and inelastic displacement demands of mid-rise RC frame buildings considering SSI. A novel concept was proposed to estimate the damage potential of a set of ground motions from the zero-amplitude axis, d_{z-a} (refs 12-14). However, none of the above studies considered the ranking of ground motions for spectral parameters of ground motions and damage to structures. The present study proposes a ranking scheme to address the above research gap through multivariate analysis.

Strong motion dataset

The ground-motion records were considered from COSMOS (Consortium of Organizations for Strong Motion Observation Systems) and PESMOS (Programme for Excellence in Strong Motion Studies). Around 35 organizations from different parts of the world contribute ground motion data

*For correspondence. (e-mail: drchenna78@gmail.com)

Table 1. Ground motion parameters, corresponding definitions and engineering applications

Ground motion parameters	Description	Characteristics	Engineering applications	Reference
Peak ground acceleration (PGA)	Maximum absolute value of acceleration time history	Amplitude	Ground motion damage index	23–25
Peak ground velocity (PGV)	Maximum absolute value of velocity time history	Amplitude	Ground motion damage index	26
Peak ground displacement (PGD)	Maximum absolute value of displacement time history	Amplitude	Design spectra	24, 27
$(V/H)_{PGA}$	Ratio of PGA values of vertical and horizontal components of ground motion	Amplitude		28
PGV/PGA	Arithmetic ratio between PGV and PGA	Frequency content	Damage measure	29
Significant duration (T_{sig})	Duration between 5% and 95% thresholds of the energy plot $T_{sig} = T_{5\%–95\%}([a(t)]^2)$	Duration	Damage index	30
Root mean square acceleration (a_{RMS})	RMS value of acceleration over significant duration $a_{rms} = \sqrt{\frac{1}{T_{sig}} \int_{t_1}^{t_2} [a(t)]^2 dt}$	Amplitude, frequency content	Damage index	31
Root mean square velocity (v_{RMS})	RMS value of velocity over significant duration $v_{rms} = \sqrt{\frac{1}{T_{sig}} \int_{t_1}^{t_2} [v(t)]^2 dt}$	Amplitude, frequency content		
Root mean square displacement (d_{RMS})	RMS value of displacement over significant duration $d_{rms} = \sqrt{\frac{1}{T_{sig}} \int_{t_1}^{t_2} [d(t)]^2 dt}$	Amplitude, frequency content		
Arias intensity (I_a)	Energy of the acceleration time history $I_a = \frac{\pi}{2g} \int_0^{T_{sig}} [a(t)]^2 dt$	Amplitude, frequency content, duration	Damage index	32
Cumulative absolute velocity (CAV)	Threshold limit for determining the operating basis ground motion $CAV = \int_0^{T_{sig}} a(t) dt$	Amplitude, frequency content, duration	Damage index	33
Characteristic intensity (I_c)	Associated with structural damage due to maximum deformation and absorbed hysteretic energy $I_c = (a_{RMS})^{1.5} (T_{sig})^{0.5}$	Amplitude, frequency content, duration	Damage index	34
Acceleration spectrum intensity (ASI)	$ASI(\xi) = \int_{0.1}^{0.5} PSA(\xi_{0.05}, T) dT$, PSA is the pseudo spectral acceleration	Amplitude, frequency content	Seismic design	35
Velocity spectrum intensity (VSI)	$VSI(\xi) = \int_{0.1}^{0.5} VSA(\xi_{0.05}, T) dT$, PSV is the pseudo spectral velocity	Amplitude, frequency content	Seismic design	36
Specific energy density (SED)	$SED = \int_0^{T_{sig}} [v(t)]^2 dt$			
Sustained maximum acceleration (SMA)	It is defined as the third highest absolute value of acceleration in the time-history record			37
Sustained maximum velocity (SMV)	It is defined as the third highest absolute value of velocity in the time-history record			37
Effective design acceleration (EDA)	It is defined as the peak acceleration value after low-pass filtering the input time history with a cut-off frequency of 9 Hz			38

Table 2. List of Indian earthquakes considered in the analysis

Earthquake	Date	Latitude	Longitude	M_w	h (km)	N
NE India*	10-09-1986	25.37	92.14	4.5	43	12
India–Burma border*	18-05-1987	25.22	94.20	5.9	49	14
India–Bangladesh border*	06-02-1988	24.66	91.56	5.8	15	18
India–Burma border*	06-08-1988	25.14	95.12	7.2	90	23
India–Burma border*	10-01-1990	24.75	95.24	6.1	119	13
Uttarkashi*	20-10-1991	30.77	78.79	7.0	10	13
Chamba*	24-03-1995	32.66	76.16	4.9	33	02
India–Burma border*	06-05-1995	24.98	95.29	6.4	117	09
India–Burma border*	08-05-1997	24.89	92.27	5.6	34	10
Chamoli*	29-03-1999	30.41	79.42	6.6	15	12
Chamoli†	14-12-2005	30.90	79.30	5.2	25	08
Uttarkashi†	22-07-2007	31.20	78.20	5.0	33	02
Nagaland†	07-07-2008	26.10	95.10	5.1	73	01
Bangladesh†	26-07-2008	24.80	90.60	4.8	39	01
India–Tibet border†	04-09-2008	30.10	80.40	5.1	10	07
Kullu†	21-10-2008	31.50	77.30	4.5	10	03
India–Myanmar border†	24-02-2009	25.90	94.30	4.8	10	03
Myanmar–India border†	11-08-2009	24.40	94.80	5.6	22	05
Sonitpur†	19-08-2009	26.60	92.50	4.9	20	02
Myanmar–Manipur border†	30-08-2009	25.40	94.80	5.3	85	03
Myanmar–Manipur border†	30-09-2009	24.30	94.60	5.9	100	03
Bhutan†	21-09-2009	27.30	91.50	6.2	08	13
Uttarkashi†	21-09-2009	30.90	79.10	4.7	13	12
Bhutan†	29-10-2009	27.30	91.40	5.2	05	05
Myanmar–India border†	29-12-2009	24.50	94.80	5.5	80	02
Bhutan†	31-12-2009	27.30	91.40	5.5	07	05
Bageswar†	22-02-2010	30.00	80.10	4.7	02	05
Tibet†	26-02-2010	28.50	86.70	5.4	28	03
Myanmar†	12-03-2010	23.00	94.50	5.6	96	01
Himachal–Punjab border†	14-03-2010	31.70	76.10	4.6	29	12
Himachal Pradesh†	28-05-2010	31.20	77.90	4.8	43	03
India–Nepal border†	06-07-2010	29.80	80.40	5.1	10	02
Meghalaya–Assam border†	11-09-2010	25.90	90.20	5.0	20	03
Manipur–Assam border†	12-12-2010	25.00	93.30	4.8	15	02
Nepal–India border†	04-04-2011	29.60	80.80	5.7	10	22
India–Nepal border†	04-05-2011	30.20	80.40	5.0	10	01
Sikkim–Nepal border†	03-06-2011	27.50	88.00	4.9	26	04
Chamoli†	20-06-2011	30.50	79.40	4.6	12	12
Sikkim–Nepal border†	18-09-2011	27.60	88.20	6.8	10	02
Sikkim–Nepal border†	18-09-2011	27.60	88.50	5.0	16	02
Haryana–Delhi border†	05-03-2012	28.70	76.60	4.9	14	13
Assam†	11-05-2012	26.60	93.00	5.4	20	02
Phek†	01-07-2012	25.70	94.60	5.8	50	03
Karbi Anglong†	10-07-2012	26.50	93.20	4.5	56	01
Kohima†	14-07-2012	25.50	94.20	5.5	35	03
Nepal–India border†	28-07-2012	29.70	80.70	4.5	10	01
Tezpur†	19-08-2012	26.70	92.50	5.0	35	01
Nepal†	23-08-2012	28.40	82.70	5.0	10	02
Chamba†	02-10-2012	32.40	76.40	4.5	10	01
Chamba†	02-10-2012	32.30	76.30	4.9	10	02
Sonitpur†	02-10-2012	26.90	92.80	5.1	35	02
Western Nepal†	11-11-2012	29.20	81.50	5.0	10	03
Uttarkashi†	27-11-2012	30.90	78.40	4.8	12	04
Western Nepal†	02-01-2013	29.40	81.10	4.8	10	02
Arunachal Pradesh†	07-01-2013	28.10	94.30	4.5	10	01
Myanmar–India border†	09-01-2013	25.40	94.90	5.9	89	05
Nepal†	09-01-2013	29.75	81.74	5.0	34	04
India–Bangladesh border†	02-03-2013	24.80	92.20	5.2	10	02
Assam†	16-04-2013	26.30	92.00	4.6	16	04
J&K–Himachal Pradesh†	01-05-2013	33.10	75.80	5.8	15	08
Lahul Spiti†	04-06-2013	32.70	76.70	4.8	18	01

(Contd)

Table 2. (Contd)

Earthquake	Date	Latitude	Longitude	M_w	h (km)	N
Chamba [†]	05-06-2013	32.80	76.30	4.5	10	01
J&K–Himachal Pradesh [†]	09-07-2013	32.90	78.40	5.1	10	01
Kangra [†]	13-07-2013	32.20	76.30	4.5	10	01
J&K–Himachal Pradesh [†]	02-08-2013	33.50	75.50	5.4	28	03
Kishtwar [†]	02-08-2013	33.40	75.90	5.2	20	02
Himachal–Punjab border [†]	29-08-2013	31.40	76.10	4.7	10	08

N , Number of ground motion records; M_w , Moment magnitude of the earthquake; h , Depth of the earthquake. *COSMOS, [†]PESMOS.

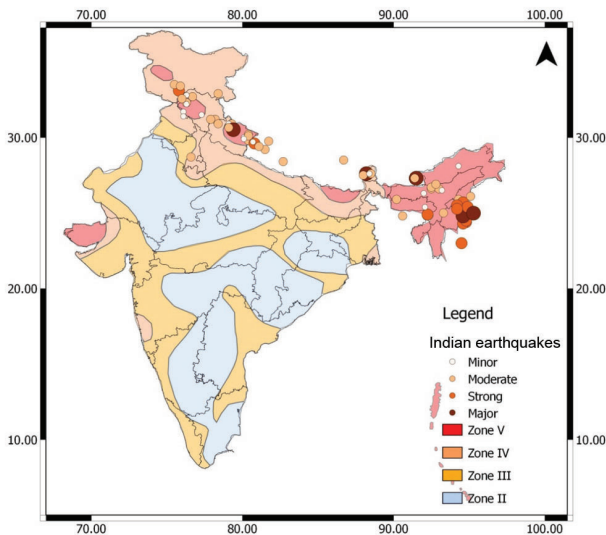


Figure 1. Location of earthquake events along the Himalayan region (data source: PEMSOS and COSMOS).

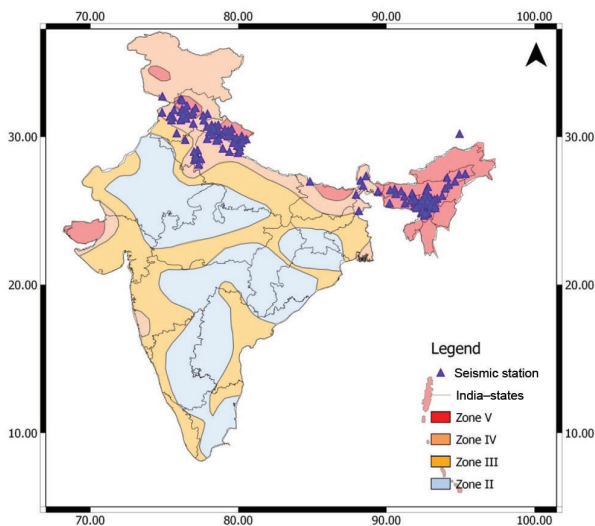


Figure 2. Location of seismic stations along the Himalayan region (data source: PEMSOS and COSMOS).

to COSMOS, and the University of California, USA has been managing the network since 1992. The Indian Institute of Technology-Roorkee (IITR) has been managing the

PESMOS network since 2004, covering the magnitude range M_w 2.3–7.8 from the Northern Himalayas to the Eastern Himalayas.

The current dataset comprises 126 ground-motion records from 10 earthquakes in the COSMOS database and 230 records from 57 earthquakes in the PEMSOS database. The database consists of magnitudes ranging from M_w 4.5 to 7.8, with a maximum hypocentral distance of 350 km. Table 2 presents a summary of the earthquake database considered in this study. Figures 1 and 2 show the location of earthquakes and seismic stations along the Himalayas respectively. Figure 3 shows the histograms of ground-motion records for the earthquake magnitude and hypocentral distances. Site effects on the ground-motion record are usually represented by the top 30 m ($V_{s,30}$) shear wave velocity of the site. The shear wave velocity profiles are unavailable for the Indian ground motion database. Hence, the site classes (namely *A*, *B* and *C*) derived by IITR are used in this study. The COSMOS site classification is based on rock/soil. Table 3 shows the classification of the site used in this study from PEMSOS. The study considers 18 GMPs and Table 1 provides a good description of each parameter. The mathematical expression for each ground motion parameter is also provided in Table 1. These parameters are calculated for each ground motion using SEISMO SIGNAL software.

Correlation analysis

Correlation analysis is a popular statistical multivariate data analysis tool for dimensionality reduction. There are two approaches in correlation analysis: (i) Pearson correlation and (ii) Spearman correlation. Pearson correlation analysis is widely used and the coefficient ranges from -1 to $+1$. Table 4 shows the variation of Pearson correlation coefficients (with which most researchers would probably agree). The Pearson correlation coefficient is computed as follows

$$r = \frac{SP_{xy}}{\sqrt{SS_x SS_y}}, \quad (1)$$

where SP is covariance and SS is standard deviation.

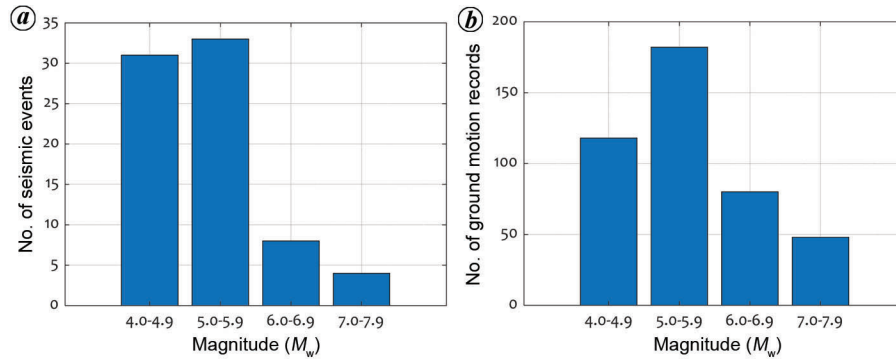


Figure 3. *a*, Number of seismic events vs magnitude of an earthquake. *b*, Number of earthquake ground-motion records.

Table 3. Site classification of soil types according to PESMOS

Soil description	$V_{s,30}$ range (m/s)	Class
Firm/hard rock	700–1620	A
Soft to firm rock	375–700	B
Soil	200–375	C

Table 4. Conventional approach to interpret the correlation coefficients

Range of correlation coefficients	Classification
0.00–0.10	Negligible correlation
0.10–0.39	Weak correlation
0.40–0.69	Moderate correlation
0.70–0.89	Strong correlation
0.90–1.00	Very strong correlation

$$SS_x = \sum X^2 - \frac{(\sum X)^2}{n}; SS_y = \sum Y^2 - \frac{(\sum Y)^2}{n};$$

$$SP_{xy} = \sum XY - \frac{(\sum X)(\sum Y)}{n},$$

where X and Y are variables of the sample and n is a number of samples.

Pearson correlation analysis was used to determine the coefficients for the selected GMPs. From the Indian seismic dataset that was considered in the analysis, the parameter root mean square acceleration (A_{rms}) had a very strong correlation with sustained maximum acceleration (SMA) (0.925), effective design accelerate (EDA) (0.929) and a strong correlation with root mean square velocity (V_{rms}) (0.737), I_c (0.887), acceleration spectrum intensity (ASI) (0.823). None of the parameters had a very strong correlation with V_{rms} . I_c strongly correlated with SMA (0.966) and EDA (0.917). ASI, velocity spectrum intensity (VSI) and SMA had a very strong correlation with EDA (0.93), SMV (0.916) and EDA (0.943) respectively. A very strong correlation between I_c and SMA (0.966) was observed among all parameters. Similarly, a very poor correlation was obser-

ved between duration and V_{rms} (0.019). Also, the amplitude parameters such as peak ground acceleration (PGA), peak ground velocity (PGV) and peak ground displacement (PGD) had a weak correlation with the other parameters. Table 5 provides a summary of correlation coefficients for all considered ground motion parameters.

Modelling of buildings

The analysis considered four types of buildings: low-rise, mid-rise, high-rise and tall. The height of each floor and storey thickness was maintained as 3 and 0.15 m respectively. The buildings considered in the analysis were classified as follows

Tall buildings: 0.1–0.59 Hz (1.7–10 sec).

High-rise buildings: 0.6–1.59 Hz (0.62–1.7 sec).

Mid-rise buildings: 1.6–3.29 Hz (0.3–0.62 sec).

Low-rise buildings: 3.3–10 Hz (0.1–0.3 sec).

The fundamental period of low-rise, mid-rise, high-rise and tall buildings was 0.3, 0.62, 1.64 and 2.0 sec respectively.

The general dynamic equilibrium equation for a building is given below.

$$[M]\{\Delta\ddot{U}\} + [C]\{\Delta\dot{U}\} + [K]\{\Delta U\} = -[M]\{\ddot{U}_g\}, \quad (2)$$

where $[M]$, $[C]$, $[K]$ are mass, damping and nonlinear stiffness matrices respectively; ΔU and its derivatives are the incremental displacement, velocity and acceleration vectors respectively. The Newmark’s β method was used to solve eq. (2) (ref. 15).

Ranking of ground motions

Few studies have been done on ranking Indian, Japanese and the USA ground motions through principal component

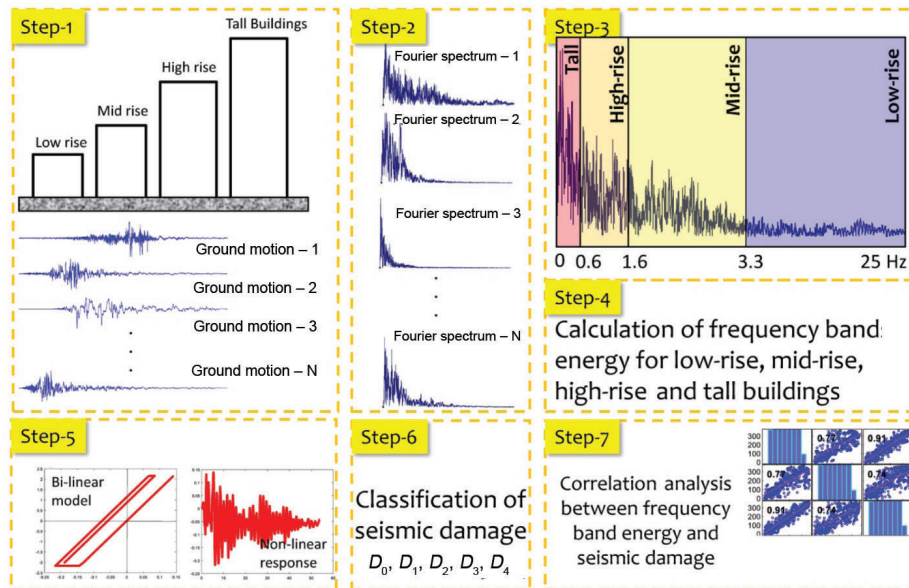


Figure 4. Schematic diagram of correlation analysis done in this study.

analysis (PSA)^{12,16,17}. From the above studies, the damage was estimated through the zero-amplitude axis and the ranking of damage of buildings has not been studied using damage models. The present study evaluated the seismic damage potential and ranking of Indian ground motions, viz. energy ranking, damage ranking and risk ranking. The ground motion records listed in Table 2 were converted into Fourier amplitude spectrum for analysis. Each spectrum was divided into four frequency bands based on the height of the building. Figure 4 (step 3) shows a schematic diagram of the frequency band.

Detailed analysis for estimating energy, damage and risk rankings of the Indian ground motions is given below.

Energy ranking

A MATLAB script was written to calculate the energy of each ground motion (E_{acc}) of each frequency band.

$$E_{acc} = \frac{1}{2\pi} \int_0^t |X(\omega)|^2 d\omega; X(\omega) = \int_0^t X(t).e^{-i\omega t} dt, \quad (3)$$

where $X(t)$ is the ground acceleration time-history record and $X(\omega)$ is the ground acceleration in frequency. The maximum PGA of 0.35 g was recorded at Gopeswar station Uttarakhand, about 15 km from the epicentre of the 1999 Chamoli earthquake. It was observed that the ground motion record at Gopeswar station had received the highest energy in frequency bands of high-rise and tall buildings and was also subjected to slight damage. On the other hand, another Tehri station located 110 km away from the epicentre of the same earthquake recorded a PGA of 0.053 g. Exten-

sive damage and collapse were observed for high-rise and tall buildings respectively, and low energy in the frequency bands of the above buildings. It indicates that high PGA and high energy may not result in more damage to a structure, and it is affected by the predominant frequency of ground motion. Further, the study extended to quantify the ranking of damage, as energy ranking is not sufficient to estimate the behaviour of buildings.

Damage ranking

Four buildings were considered to estimate seismic damage. The fundamental periods of the buildings were $T_L = 0.38$ sec, $T_M = 0.62$ sec, $T_H = 1.64$ sec and $T_T = 2.0$ sec, where the subscripts L, M, H and T indicate low-rise, mid-rise, high-rise and tall buildings respectively. The subscripts D and E represent the ranking of damage and energy in the frequency band of the above buildings respectively. These buildings were subjected to ground motion considered in the analysis to obtain the nonlinear displacement time-history response. A MATLAB script was written to calculate the nonlinear displacement response of the considered buildings. An elastic-perfectly-plastic (EPP) model was used in this analysis. A detailed description for calculating the displacement response is provided by Paz¹⁸.

A PGA of 0.35 g was recorded at Gopeswar station during the 1999 Chamoli earthquake. Figure 5 shows the Fourier amplitude spectrum. The maximum nonlinear displacement response for low-rise, mid-rise, high-rise and tall buildings was 0.025, 0.078, 0.319 and 0.275 m respectively. Among the above displacement responses, a maximum nonlinear displacement of 0.319 m was observed for a building with a fundamental period of 1.64 sec. Figure 5 also shows the

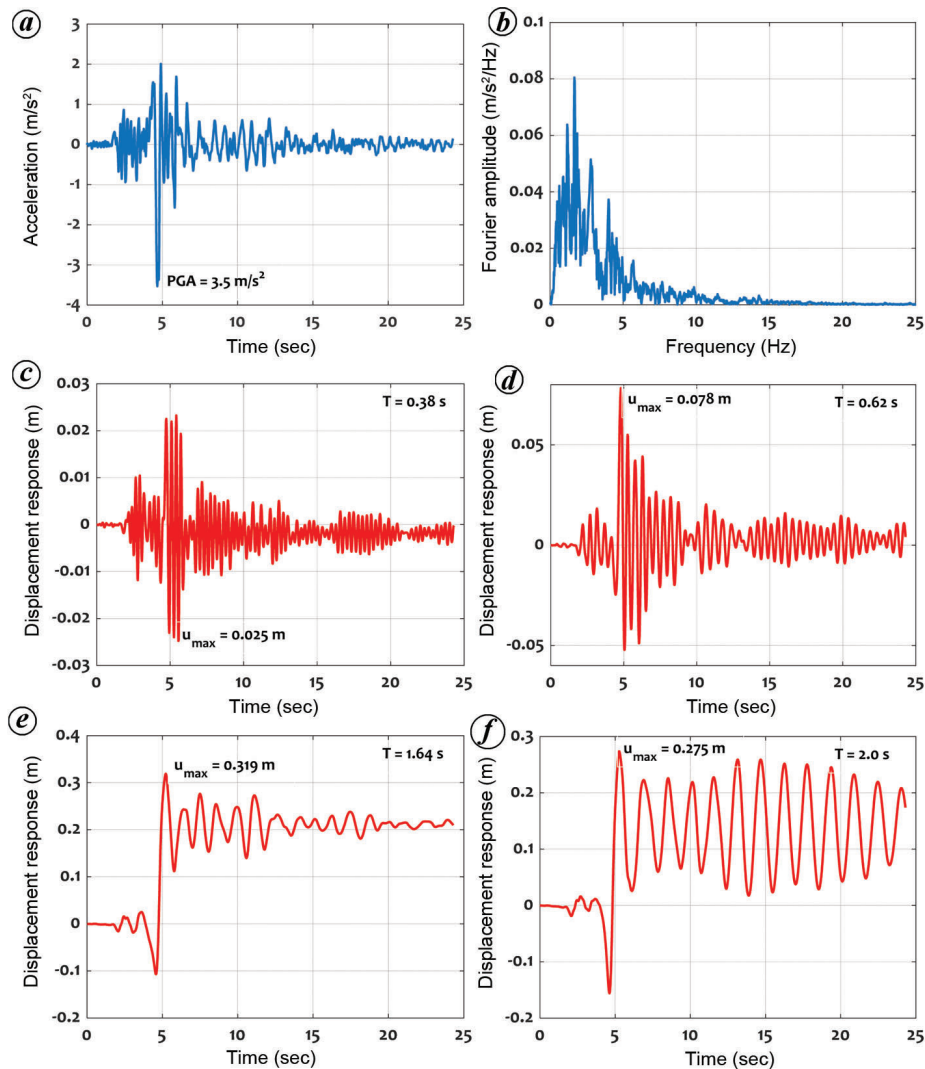


Figure 5. Nonlinear displacement time-history response of buildings with various fundamental periods. (a) Ground motion record of Gopewar station, 1999 Chamoli earthquake. (b) Fourier amplitude spectrum of the corresponding ground motion record. (c) Nonlinear response of the buildings with time periods: $T = 0.38$ sec, (d) $T = 0.62$ sec, (e) $T = 1.64$ sec and (f) $T = 2.0$ sec.

Table 6. Classification of seismic damage¹⁹

Damage index	Classification of damage
<0.2	No damage
0.2–0.4	Slight damage
0.4–0.6	Moderate damage
0.6–0.8	Extensive damage
0.8–1.0	Collapse

nonlinear displacement response of the buildings. The seismic damage of each building type subjected to the ground motion was further classified into five categories, namely no damage (D_0), slight damage (D_1), moderate damage (D_2), extensive damage (D_3) and collapse (D_4) (Table 6). Park and Ang¹⁹ model was considered for the estimating seismic damage to the buildings.

Validation of seismic damage indices

To validate the above damage classification, each building type considered in the analysis was subjected to the ground motion of the 1999 Chamoli earthquake recorded at Chamoli station. The Park–Ang damage model was used to estimate seismic damage to the buildings

$$D = \frac{x_m - x_y}{x_u - x_y} + \beta \frac{EH}{Q_y x_u}, \quad (4)$$

where x_m is the maximum displacement that a building would be subjected to during base excitation, x_u ($= \mu x_y$, where μ is the ductility and x_y is the yield displacement) is the ultimate displacement of the system under monotonic loading, β is the effect of cyclic loading on structural damage, EH is

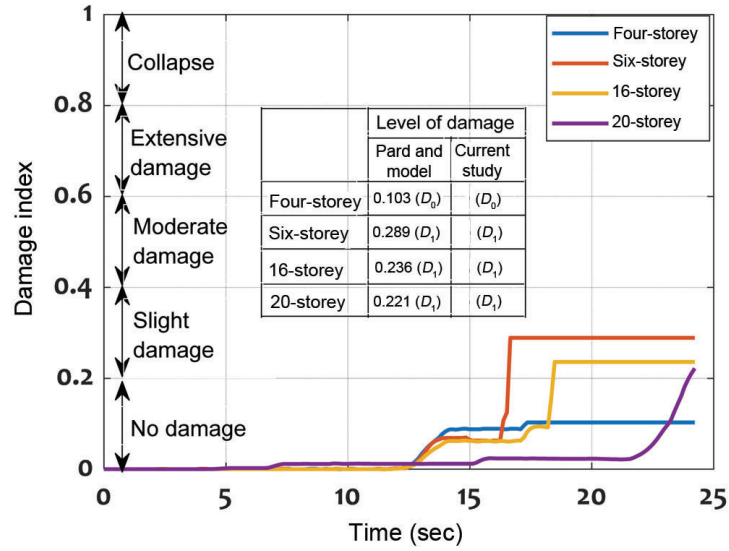


Figure 6. Damage indices of four-, six-, 16- and 20-storeyed buildings subjected to Gopewar ground motion, 1999 Chamoli earthquake and a comparison with the damage model proposed by Ghobarah³⁸.

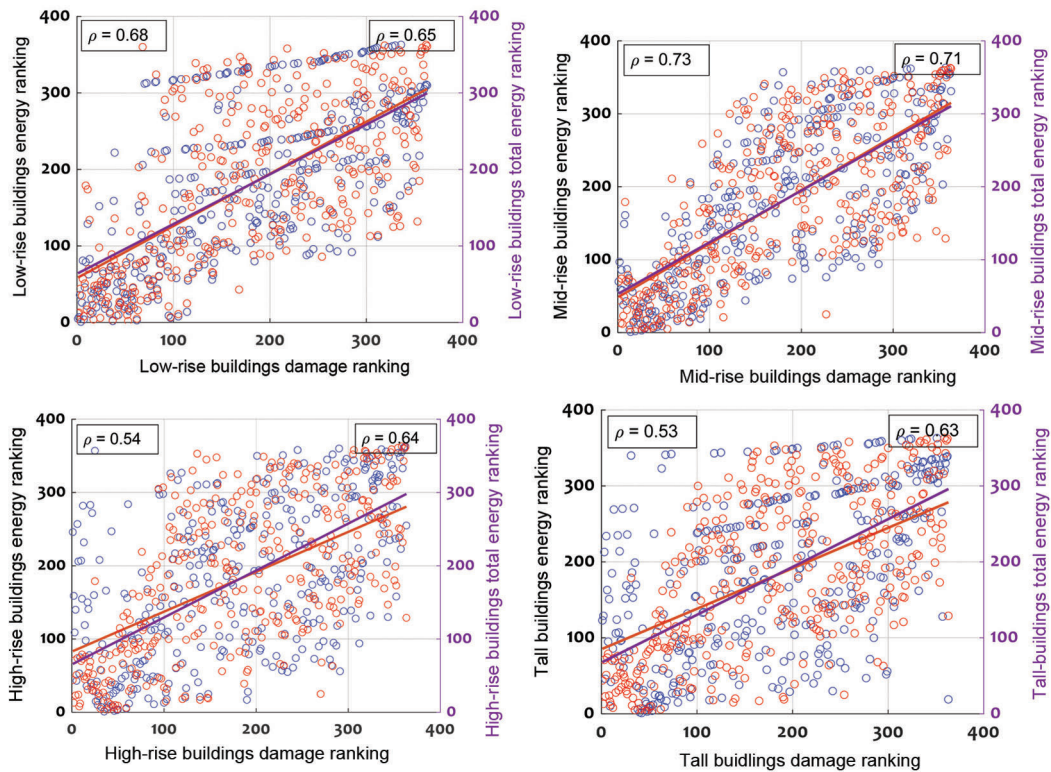


Figure 7. Pearson correlation between $T_D - T_E$, $H_D - H_E$, $M_D - M_E$, $L_D - L_E$ and total energy. (The letters L, M, H and T indicate low-rise, mid-rise, high-rise and tall buildings respectively. The subscript D and E represent damage and energy respectively).

the total energy dissipation in the structure during excitation and Q_y is the yield strength of the structure^{19,20}.

The RC buildings were modelled using the tool inelastic damage analysis of reinforced concrete (IDARC) tool and the inelastic displacement responses were evaluated through

nonlinear time history analysis²¹. The cumulative damage curves were plotted against time for the buildings (Figure 6). From the results, it can be observed that the Park and Ang damage index (DI) is less than 0.2 (no damage) for low-rise buildings and greater than 0.2 (slight damage) for

Table 7. Comparison of correlation coefficients between the present study and a past study

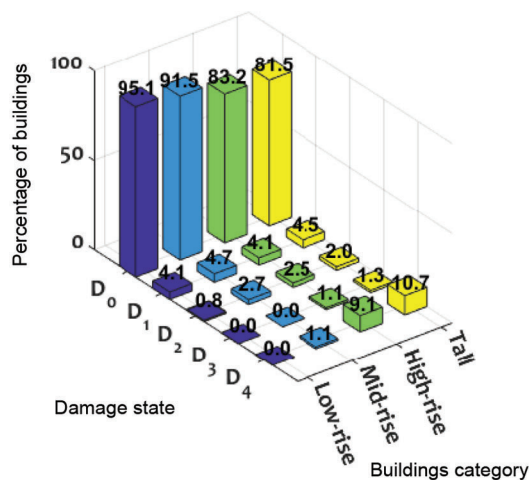
Zero amplitude axis (d_{z-a})	1.00				
Damage for low-rise building (L_D)	0.50	1.00			
Damage for mid-rise building (M_D)	0.52	0.81	1.00		
Damage for high-rise building (H_D)	0.57	0.70	0.78	1.00	
Damage for tall building (T_D)	0.58	0.71	0.77	0.94	1.00
	d_{z-a}	L_D	M_D	H_D	T_D

Bold indicates past study¹⁴.

Table 8. Percentage-wise damage state of buildings subjected to a set of ground motions

Damage category	Low-rise (%)	Mid-rise (%)	High-rise (%)	Tall buildings (%)
D_0	95.1 (8559)	91.5 (5490)	83.2 (3328)	81.5 (815)
D_1	4.1 (369)	4.7 (282)	4.1 (164)	4.5 (45)
D_2	0.8 (72)	2.7 (162)	2.5 (100)	2.0 (20)
D_3	0.0 (0)	0.0 (0)	1.1 (44)	1.3 (13)
D_4	0.0 (0)	1.1 (66)	9.1 (364)	10.7 (107)
$D_0 - D_4$	100 (9000)	100 (6000)	100 (4000)	100 (1000)

Values in brackets are the number of buildings affected to different states of seismic damage.

**Figure 8.** Buildings subjected to different damage states.

mid-rise, high-rise and tall buildings subjected to ground motion.

Correlation between damage and energy rankings

The linear Pearson correlation coefficients were computed between damage, energy and total energy of buildings to confirm the trend of parameters and their influence on total energy ranking. A scatter plot was drawn between each category of damage to the buildings and energy ranking (Figure 7). It can be noticed that damage for low-rise building (L_D), high-rise building (H_D) and tall building (T_D) moderately correlate with the total energy, while M_D strongly correlates with the total energy. Also, L_D and energy for low-rise building (L_E) (0.68), H_D and energy for high-rise building (H_E) (0.54) and T_D and energy for tall building

(T_E) (0.53) are moderately correlated, while a strong correlation is observed between M_D and M_E (0.73) using the Pearson correlation coefficient.

Validation of damage ranking

A correlation analysis was done to validate the damage ranking with d_{z-a} (ref. 14). This is defined as the location of the ground motion farther from the zero amplitude axis leading to greater damage potential. Our analysis considered the damage ranking of buildings to validate the damage potential of ground motions according to d_{z-a} . For this purpose, correlation analysis was done between the damage ranking of each building and the damage potential of ground motion proposed by Podili *et al.*¹⁴. The correlation coefficients were estimated and tabulated (Table 7). The results showed a moderate correlation between damage potential rankings according to d_{z-a} . Whereas the damage rankings for various frequency bands of buildings ranged from strong to very strong correlations. Damage ranking plays a vital role in the decision to retrofit buildings. To formulate Government policies on retrofitting buildings, it is necessary to estimate the risk of a region. Hence, further analysis was carried out to assess seismic risk in the high-seismic zone.

Seismic risk ranking

Hypothetical data consisting of a city in seismic zone-V with a population of one lakh and 20,000 buildings were considered for the analysis. It was assumed that 5%, 20%, 30% and 45% of the buildings were tall, high-rise, mid-rise and low-rise respectively. The buildings were subjected to a set of considered Indian ground motions to estimate the damage state of each building type. Figure 8 and Table 8

show the damage state of each building category. It was observed that around 10% of high-rise and tall buildings collapsed, and more than 80% of the buildings were undamaged. The low-rise buildings did not suffer extensive damage and collapse. Around 1%, 9% and 11% of mid-rise, high-rise and tall buildings respectively, experienced a collapse due to the considered ground motions. As a result, more than 2600 people are expected to be homeless. The Government needs to take policy decisions on retrofitting buildings whose damage state is extensive.

Conclusion

A three-ranking procedure, namely energy ranking, damage ranking and seismic risk ranking has been proposed for different types of buildings subjected to Indian ground motion records. A correlation analysis was done between damage to the buildings, energy and total energy to confirm the trend of parameters and their influence on total energy ranking. From the energy ranking, high PGA or high total energy alone may not cause damage to the structure. However, it is affected by the predominant frequency of ground motion. The energy of the ground motion ranking may be useful for geophysical studies in a region. From damage ranking, it can be concluded that seismic damage to low-rise buildings correlates moderately with A_{rms} , I_c , SMA and EDA. Also, a weak correlation is observed between seismic damage of high-rise, tall buildings and $(V/H)_{PGA}$, A_{rms} . Thus it concluded that L_D , H_D and T_D moderately correlate with the total energy. The damage and seismic risk rankings may help change Government policies for retrofitting buildings. For future studies, other parameters such as ground shaking, collateral hazard, floor-space index, life-threatening factors and economic loss-induced factors must be considered while estimating the seismic risk of a city, as proposed by Pradeep and Murty²². Also, the present analysis did not consider the actual built environment of a city or region.

Conflict of interest: The authors declare no conflict of interest.

1. Yakut, A. and Yilmaz, H., Correlation of deformation demands with ground motion intensity. *J. Struct. Eng. (ASCE)*, 2008, **134**, 1818–1828; [https://doi.org/10.1061/\(ASCE\)0733-9445\(2008\)134:12\(1818\)](https://doi.org/10.1061/(ASCE)0733-9445(2008)134:12(1818)).
2. Cao, V. V. and Ronagh, H. R., Correlation between parameters of pulse-type motions and damage of low-rise RC frames. *Earthq. Struct.*, 2014, **7**, 365–384; <https://doi.org/10.12989/eas.2014.7.3.365>.
3. Ozmen, H. B. and Inel, M., Damage potential of earthquake records for RC building stock. *Earthq. Struct.*, 2016, **10**, 1315–1330; <https://doi.org/10.12989/eas.2016.10.6.1315>.
4. Elenas, A., Interdependency between seismic acceleration parameters and the behavior of structures. *Soil Dyn. Earthq. Eng.*, 1997, **16**, 317–322; [https://doi.org/10.1016/S0267-7261\(97\)00005-5](https://doi.org/10.1016/S0267-7261(97)00005-5).
5. Elenas, A., Correlation between seismic acceleration parameters and overall structural damage indices of buildings. *Soil Dyn. Earthq. Eng.*, 2000, **20**, 93–100; [https://doi.org/10.1016/S0267-7261\(00\)00041-5](https://doi.org/10.1016/S0267-7261(00)00041-5).
6. Meskouris, K., Kratzig, W. B. and Hanskotter, U., Nonlinear computer simulations of seismically excited wall-stiffened, reinforced concrete buildings. In Proceedings of the Second European Conference on Structural Dynamics: EURO DYN, Balkema, Rotterdam, The Netherlands, 1999, pp. 49–53.
7. Alvanitopoulos, P. F. and Elenas, A., Interdependence between damage indices and ground motion parameters based on Hilbert–Huang transform. *Meas. Sci. Technol.*, 2010, **21**(2), 71–83; <https://doi.org/10.1088/0957-0233/21/2/025101>.
8. Elenas, A., Intensity parameters as damage potential descriptors of earthquakes. In Proceedings of the Third International Conference on Computational Methods in Structural Dynamics and Earthquake Engineering: COMPDYN, 2013, pp. 327–334.
9. Elenas, A. and Meskouris, K., Correlation study between seismic acceleration parameters and damage indices of structures. *Eng. Struct.*, 2001, **23**, 698–704; [https://doi.org/10.1016/S0141-0296\(00\)00074-2](https://doi.org/10.1016/S0141-0296(00)00074-2).
10. Konstantinos, K., Manthos, P., Asimina, A. and Konstantinos, M., Correlation between structure specific ground motion intensity measures and seismic response of 3D RC buildings. In Proceedings of the Third International Conference on Earthquake Engineering and Seismology, Istanbul, Turkey, 2014.
11. Kamal, M. and Inel, M., Correlation between ground motion parameters and displacement demands of mid-rise RC buildings on soft soils considering soil–structure interaction. *Buildings*, 2021, **11**, 125; <https://doi.org/10.3390/buildings11030125>.
12. Iyengar, R. N. and Proadhan, K. C., Classification and rating of strong motion earthquake records. *Earthq. Eng. Struct. Dyn.*, 1983, **11**, 415–426; <https://doi.org/10.1002/eqe.4290110308>.
13. Bhargavi, P. and Raghukanth, S. T. G., Rating damage potential of ground motion records. *Earthq. Eng. Vib.*, 2019, **18**, 233–254; <https://doi.org/10.1007/s11803-019-0501-1>.
14. Podili, B. and Raghukanth, S. T. G., Rating of Indian ground motion records. *Nat. Haz.*, 2019, **96**, 53–95; <https://doi.org/10.1007/s11069-018-3530-6>.
15. Chopra, A. K., *Dynamics of Structures: Theory and Applications to Earthquake Engineering*, Prentice-Hall, New Jersey, USA, 1995.
16. Bhargavi, P. and Raghukanth, S. T. G., Ground motion parameters for the 2011 great Japan Tohoku earthquake. *J. Earthq. Eng.*, 2017, **23**, 1363–2469; <https://doi.org/10.1080/13632469.2017.1342292>.
17. Bhargavi, P. and Raghukanth, S. T. G., Ground motion prediction equations for higher order parameters. *Soil Dyn. Earthq. Eng.*, 2019, **118**, 98–110; <https://doi.org/10.1016/j.soildyn.2018.11.027>.
18. Paz, M. and William, L., *Structural Dynamics – Theory and Computation*, Kluwer Academic Publishers, Massachusetts, USA, 2004.
19. Park, Y. J. and Ang, A. H. S., Mechanistic seismic damage model for reinforced concrete. *J. Struct. Eng. (ASCE)*, 1985, **111**, 722–739; [https://doi.org/10.1061/\(ASCE\)0733-9445\(1985\)111:4\(722\)](https://doi.org/10.1061/(ASCE)0733-9445(1985)111:4(722)).
20. Kunnath, S. K., Reinhorn, A. M. and Park, Y. J., Analytical modeling of inelastic seismic response of RC structures. *J. Struct. Eng. (ASCE)*, 1990, **116**, 996–1017; [https://doi.org/10.1061/\(ASCE\)0733-9445\(1990\)116:4\(996\)](https://doi.org/10.1061/(ASCE)0733-9445(1990)116:4(996)).
21. Reinhorn, A. M., Sivaselvan, M., Kunnath, S. K., Valles, R. E., Madan, A., Park, Y. J. and Lobo, R., IDARC2D Version 7.0: A Program for the Inelastic Damage Analysis of Structures, University at Buffalo, New York, USA, 2009.
22. Pradeep, K. R. and Murty, C. V. R., Earthquake disaster risk index – a simple method for assessing relative risk in a country. In Proceedings of 17th World Conference on Earthquake Engineering (17WCEE), Sendai, Japan, 2020.
23. Gutenberg, B. and Richter, C. F., Earthquake magnitude: intensity, energy and acceleration. *Bull. Seismol. Soc. Am.*, 1942, **32**, 163–191; <https://doi.org/10.1785/BSSA0320030163>.
24. Newmark, N. M. and Hall, W. J., *Procedures and Criteria for Earthquake Resistant Design*, Building Science Series, National Bureau of Standards, Washington DC, USA, 1973.

25. Parvez, I. A., Vaccari, F. and Panza, G. F., A deterministic seismic hazard map of India and adjacent areas. *Geophys. J. Int.*, 2003, **155**, 489–508; <https://doi.org/10.1046/j.1365-246X.2003.02052.x>.
26. Rosenblueth, E., Probabilistic design to resist earthquakes. *J. Eng. Mech. Div. ASCE*, 1964, **90**, 189–219; <https://doi.org/10.1061/JMCEA3.0000536>.
27. Priestly, M. J. N., Myths and fallacies in earthquake engineering – conflicts between design and reality. *Bull. NZNSEE*, 1993, **26**, 329–341.
28. Kramer, S. L., *Geotechnical Earthquake Engineering*, Prentice-Hall, New Jersey, USA, 1996.
29. Zhu, T. J., Tso, W. K. and Heidebrecht, A. C., Effects of peak A/V ratio on structural damage. *J. Struct. Eng. (ASCE)*, 1988, **114**, 1019–1037; [https://doi.org/10.1061/\(ASCE\)0733-9445\(1988\)114:5\(1019\)](https://doi.org/10.1061/(ASCE)0733-9445(1988)114:5(1019)).
30. Trifunac, M. D. and Brady, A. G., A study on the duration of strong earthquake ground motion. *Bull. Seismol. Soc. Am.*, 1975, **65**, 581–626; <https://doi.org/10.1785/BSSA0650030581>.
31. Housner, G. W. and Jennings, P. C., Generation of artificial earthquakes. *J. Eng. Mech. Div. ASCE*, 1964, **90**, 113–152; <https://doi.org/10.1061/JMCEA3.0000448>.
32. Arias, A., A measure of earthquake intensity. In *Seismic Design for Nuclear Power Plants* (ed. Hansen, R. J.), MIT Press, Cambridge, USA, 1970, pp. 438–483.
33. EPRI, A criterion for determining exceedance of the operating basis earthquake, EPRI NP-5930, Electrical Power Research Institute, Palo Alto, CA USA, 1988.
34. Park, Y. J., Ang, A. H. S. and Wen, Y. K., Seismic damage analysis of reinforced concrete buildings, *J. Struct. Eng. (ASCE)*, 1985, **111**, 740–757; [https://doi.org/10.1061/\(ASCE\)0733-9445\(1985\)111:4\(740\)](https://doi.org/10.1061/(ASCE)0733-9445(1985)111:4(740)).
35. Von Thun, J. L., Rochim, L. H., Scott, G. A. and Wilson, J. A., Earthquake ground motions for design and analysis of dams. In *Earthq. Eng. Soil Dyn. II – Recent Advance in Ground Motion Evaluation*, Geotechnical Special Publication 20, ASCE, New York, USA, 1988, pp. 463–481.
36. Housner, G. W., Spectrum intensity of strong motion earthquakes. In *Proceedings of the Symposium on Earthquakes and Blast Effects on Structures*. Earthquake Engineering Research Institute, California, USA, 1952, pp. 20–36.
37. Nuttli, O. W., The relation of sustained maximum ground acceleration and velocity to earthquake intensity and magnitude. Miscellaneous Paper S-71-1, Report 16, US, Army Corps of Engineers, Waterways Experiment Station, Vicksburg, Mississippi, USA, 1979.
38. Ghobarah, A., Performance-based design in earthquake engineering: state of development. *Eng. Struct.*, 2001, **23**(8), 878–884; [https://doi.org/10.1016/S0141-0296\(01\)00036-0](https://doi.org/10.1016/S0141-0296(01)00036-0).

Received 30 March 2022; revised accepted 8 October 2022

doi: 10.18520/cs/v124/i2/190-201